Journal of Applied Electrochemistry (2005) 35:259–265
DOI 10.1007/s10800-004-6708-4
© Springer 2005

Open circuit voltage for solid polymer electrolyte/salt systems in lithium batteries

SUNG JIN PAI and YOUNG CHAN BAE*
Division of Chemical Engineering and Molecular Thermodynamics Laboratory, Hanyang University, Seoul 133-791, Korea; http://www.inchem.hanyang.ac.kr/lab/mtl/
*(*author for correspondence, e-mail: ycbae@hanyan.ac.kr)*

Received 16 October 2003; accepted in revised form 10 November 2004

Key words: lithium battery, MDL-NR model, melting point depression, open circuit voltage, solid polymer electrolyte

Abstract

The open circuit voltage (OCV) model of the solid polymer electrolyte (SPE)/salt system in lithium batteries is established by combining concentrated solution theory with the modified double lattice–non-random (MDL-NR) model which describes the non-ideal behavior of the salt activity in the polymer electrolyte. The activity parameters are obtained from the phase diagram for the given systems and used to describe the OCV of the corresponding systems with one additional parameter, transport number, t_+^0. The proposed model agrees very well with the OCV data for various PEO/salt systems.

1. Introduction

The research and development of solid polymer electrolyte (SPE) began when Wright found ion conductivity in a PEO–alkaline metal ion complex in 1975 [1]. The conductivity then was 1×10^{-7} S cm^{-1} at room temperature. A lithium polymer battery has features such as flexibility in the shape of a cell design, leak proof electrolyte, high safety, etc., but poses the challenge of how close its electrical performance can be made to that of a liquid electrolyte cell. Therefore, various efforts have been made to improve the ionic conductivity of the SPE. Recently, such efforts have also included the development of gelled SPE and porous SPE, especially in the consideration of its practical application, in particular the use at low temperature. The ionic conductivity of such SPEs now reaches 1×10^{-3} S cm^{-1} at room temperature [2].

There has been much work on modeling of electrolytes to predict their properties, for example, ionic conductivity, apparent salt diffusion coefficient, glass transition temperature, etc. A macroscopic model of the transport process has many useful aspects. Modeling may be used to understand [3] and describe the behavior of batteries [4, 5] if their transport properties are known, and also for the optimization of the battery design [6].

To describe the transport processes in the electrolyte, there are two classes according to the theory used: the dilute and the concentrated solution theory [7]. The dilute theory is valid when non-ionic interactions take place and when the electrolyte is ideal. Although battery SPEs generally have high salt concentration, with non-ideal behavior and strong ionic interactions present, the theory for dilute electrolytes has been used in several methods proposed [8–18]. The theory for concentrated electrolytes, on the other hand, remains valid from zero to high concentrations, taking non-ideality and ionic interactions into account. Methods based on this theory are preferred, because they result in a full description of the ionic transport parameters that can be used for the battery design.

In the modeling of electrolyte, the cationic transport number, t_+^0, has been found to be a critical property for batteries based on SPEs [19]. However, t_+^0 has proven difficult to measure correctly for SPEs and there are few characterization methods available. As a result of the different methods used, significant variations in transport properties can be found for similar SPEs, especially for the cationic transport number. While calculating the transport number, it is important to know the salt activity coefficient, $f_\pm$, in order to relate the transport number to a concentration gradient.

The activity coefficient of salt in polymer has been well established since Flory developed the lattice theory [20]. The study of phase diagrams appears to be an appropriate descriptive approach for a better understanding of conductivity, stability and mechanical properties, and as such have been the objective of several studies to determine the domain of existence as a function of salt type, composition and temperature. Smith and Pennings [21] showed that, according to Flory's melting point depression theory, a eutectic point might occur in an athermal polymer/diluent system if the melting point of a diluent is not too low in

comparison with that of the polymer. For example, Gryte et al. [22] reported crystallization characteristics of PEO/glutaric acid system, and Myasnikova et al. [23] provided the phase diagram of the PEO/resorcinol system in which resorcinol molecules form hydrogen bonds to the polymer chain. Recently the Bae group [24–26] has investigated this subject using various thermodynamic models that describe phase behaviors of SPE/salt systems. These theories can describe various effects (pressure, free volume, etc) and agree with experimental data quite remarkably.

In this study, we combine the OCV model [27] with the thermodynamic model that describes the salt activity of the given systems. The salt activity explains deviations from the ideal behavior. To describe the non-ideality of the systems, we employ the MDL–NR [28] model which explains the phase behavior of the real systems comparatively well. Comparison of a theoretical OCV prediction for PEO/$LiCF_3SO_3$ and PEO/$ZnBr_2$ systems with experimental data of the PEO/$NaCF_3SO_3$ system is made to examine physical reliability.

2. Model description

To describe the OCV of a concentration cell that consists of two identical electrodes and PEO/salt electrolyte, the variation of voltage in the electrolyte is calculated from the concentrated solution theory of the transport process. In this work, three theoretical aspects are taken into account:

1. The concentrated solution theory to express OCV.
2. The MDL-NR model to describe the non-ideality of the SPE system.
3. Flory's melting point depression theory [20] to correlate chemical potential to experimental melting temperature data.

We assume that the salt is a particle to consider a salt effect of the free energy of mixing in the calculation of phase behavior.

2.1. *Cell voltage model from the concentrated solution theory*

The flux density of each dissolved species restricted to dilute solutions is given by

$$N_i = -z_i u_i F c_i \nabla\Phi - D_i \nabla c_i + c_i \mathbf{v} \tag{1}$$

In a concentrated solution such as SPE, this flux equation fails even in ternary solutions of non-electrolyte, since in such solutions there are two independent concentration gradients and the diffusion flux of each species can be affected by both concentration gradients. Equation (1) can be replaced by the multi-component diffusion equation by Maxwell–Stefan [29]

$$c_i \nabla \mu_i = \sum_i K_{ij}(v_j - v_i) = RT \sum_j \frac{c_i c_j}{c_T D_{ij}}(v_j - v_i) \qquad (i \neq j,\ D_{ij} = D_{ji}) \tag{2}$$

where μ_i is the electrochemical potential of species i and K_{ij} is the friction coefficient or the interaction coefficient. v_i is the velocity of species i, an average velocity for the species but not the velocity of individual molecules. R and T are the gas constant and temperature of the system, respectively. c_T is the total concentration, and D_{ij} is a diffusion coefficient describing the interaction of species i and j. These diffusion coefficients are simply parameters that can replace the drag coefficients K_{ij}:

$$K_{ij} = \frac{RTc_i c_j}{c_T D_{ij}} \tag{3}$$

The gradient in electrochemical potential, $\nabla\mu_i$, is used as the driving force in Equation (2) including gradients both in potential and concentration. For species i, it follows from [30]

$$\nabla\mu_i = RT\nabla \ln a_i + z_i F \nabla\Phi \tag{4}$$

where $\nabla\Phi$ is the electrostatic potential difference and a_i is an activity which is supposed to be independent of the electrical state of the phase. F is the Faraday constant and z_i is the charge of species i. $\nabla\Phi$ is directly measurable as the voltage difference of two similar electrodes positioned in the electrolyte.

The property used in this study is the OCV of the concentration cell. To enable calculations, it is necessary to adopt an expression for the potential as a function of the concentration profile. Equations (2) and (4) can be combined and solved for the potential difference, Equation (5). A full derivation can be found elsewhere [7].

$$\nabla\Phi = \frac{vRT}{z_+ v_+ F}\nabla\left[\left(1 + \frac{\mathrm{d}\ln f_\pm}{\mathrm{d}\ln c_s}\right)(1 - t_+^0)\ln c_s\right] - \frac{\mathbf{i}}{\kappa} \tag{5}$$

where $f_\pm$ is the mean activity coefficient; c_s is the concentration of the salt; t_+^0 is the transport number of the cation; $\mathbf{i}$ is the current density; κ is the ionic conductivity of the salt. From this equation, we see that if $\mathbf{i} = 0$ we have the expression for the OCV of a concentration cell, and the thermodynamic factor in the first parenthesis can be expressed simply as the differentiation of the salt activity:

$$\nabla\Phi = \frac{vRT}{z_+ v_+ F}\nabla\left[\left(\frac{\mathrm{d}\ln a_\pm}{\mathrm{d}\ln c_s}\right)(1 - t_+^0)\ln c_s\right] \tag{6}$$

Thus the potential of this cell can be used to determine t_+^0 if the activity of salt is known.

2.2. *Modified double lattice–non-random (MDL-NR) model*

In the previous work [28], we established the MDL-NR model by introducing the non-randomness factor in the MDL model proposed by Oh et al. [31]. In this model, the expression for the Helmholtz energy of mixing for binary polymer solutions is calculated as a sum of two contributions

$$\left(\frac{\Delta A}{kT}\right) = \left(\frac{\Delta A}{kT}\right)_{\mathrm{MDL}} + \left(\frac{\Delta A}{kT}\right)_{\mathrm{NR}} \tag{7}$$

The first term of Equation (7) explains the random mixing of polymer/salt systems by using the MDL model. Since the model has the secondary lattice which takes into account the specific interaction between particles, it can describe more kinds of phase diagram than comparatively simple Flory–Huggins model [31]. The chemical potential [28] is given by

$$\begin{aligned}\frac{\Delta\mu_1}{kT} = {} & \ln(1-\phi_2) - r_1\left(\frac{1}{r_2}-\frac{1}{r_1}\right)\phi_2 \\ & + r_1\left[C_\beta\left(\frac{1}{r_2}-\frac{1}{r_1}\right)^2 + \left(\left(\frac{1}{r_2}-\frac{1}{r_1}\right) + C_\gamma\tilde{\varepsilon}\right)\tilde{\varepsilon}\right. \\ & \left. + \left(2+\frac{1}{r_2}\right)\tilde{\varepsilon}\right]\phi_2^2 - 2r_1\left[\left(\left(\frac{1}{r_2}-\frac{1}{r_1}\right) + C_\gamma\tilde{\varepsilon}\right)\tilde{\varepsilon}\right. \\ & \left. + C_\gamma\tilde{\varepsilon}^2\right]\phi_2^3 + 3r_1C_\gamma\tilde{\varepsilon}^2\phi_2^4 \end{aligned} \tag{8}$$

and

$$\begin{aligned}\frac{\Delta\mu_2}{kT} = {} & \ln\phi_2 + r_2\left[\left(\frac{1}{r_2}-\frac{1}{r_1}\right) + C_\beta\left(\frac{1}{r_2}-\frac{1}{r_1}\right)^2\right. \\ & \left. + \left(2+\frac{1}{r_2}\right)\tilde{\varepsilon}\right] - r_2\left[\left(\frac{1}{r_2}-\frac{1}{r_1}\right)\right. \\ & \left. + 2\left(\left(\frac{1}{r_2}-\frac{1}{r_1}\right) + C_\gamma\tilde{\varepsilon}\right)\tilde{\varepsilon}\right. \\ & \left. + 2C_\beta\left(\frac{1}{r_2}-\frac{1}{r_1}\right)^2 + 2\left(2+\frac{1}{r_2}\right)\tilde{\varepsilon}\right]\phi_2 \\ & + r_2\left[4\left(\left(\frac{1}{r_2}-\frac{1}{r_1}\right) + C_\gamma\tilde{\varepsilon}\right)\tilde{\varepsilon} + \left(2+\frac{1}{r_2}\right)\tilde{\varepsilon}\right. \\ & \left. + C_\beta\left(\frac{1}{r_2}-\frac{1}{r_1}\right)^2 + 3C_\gamma\tilde{\varepsilon}^2\right]\phi_2^2 \\ & - r_2\left[6C_\gamma\tilde{\varepsilon}^2 + 2\left(\left(\frac{1}{r_2}-\frac{1}{r_1}\right) + C_\gamma\tilde{\varepsilon}\right)\tilde{\varepsilon}\right]\phi_2^3 \\ & + 3r_2C_\gamma\tilde{\varepsilon}^2\phi_2^4 \end{aligned} \tag{9}$$

where ϕ_i is the segment fraction of component i, $\phi_i = N_i r_i / N_r$, $N_r\left(=\sum_i^m N_i r_i\right)$ is the total number of segments in the system and r_i is the segment number of component 1 (salt) and 2 (polymer). C_β and C_γ are universal constants having 0.1415 and 1.7986, respectively. Reduced interaction parameter, $\tilde{\varepsilon}$, is defined by

$$\tilde{\varepsilon} = \frac{\varepsilon}{kT} - \left[\sum_i\left(\frac{\Delta A_{\mathrm{sec},ii}}{N_{ii}kT}\right) - 2\left(\frac{\Delta A_{\mathrm{sec},ij}}{N_{ij}kT}\right)\right] \tag{10}$$

The Helmholtz free energy of mixing for the secondary lattice, $\Delta A_{\mathrm{sec},ij}$, is given by

$$\begin{aligned}\frac{\Delta A_{\mathrm{sec},ij}}{N_{ij}kT} = {} & \frac{2}{z}\left[\eta\ln\eta + (1-\eta)\ln(1-\eta)\right. \\ & \left. + \frac{zC_\alpha\delta\tilde{\varepsilon}_{ij}(1-\eta)\eta}{1+C_\alpha\delta\tilde{\varepsilon}_{ij}(1-\eta)\eta}\right] \end{aligned} \tag{11}$$

where N_{ij} is the number of *i-j* pairs, $\delta\tilde{\varepsilon}_{ij}$ is the reduced energy parameter contributed by the oriented interactions and η is the surface fraction permitting oriented interactions and C_α is a universal constant of 0.4881.

We employ Panayiotou et al.'s local composition expression [32] to describe the non-random contribution:

$$\left(\frac{\Delta\mu_i}{kT}\right)_{NR} = \frac{zq_i}{2}\ln\Gamma_{ii} \tag{12}$$

where the surface factor zq_i is calculated from

$$zq_i = r_i(z-2) + 2 \tag{13}$$

For the binary solution, the non-randomness factor between *i-j* pairs in Equation (12), Γ_{ij}, is given by

$$\Gamma_{12} = \frac{2}{1+\left[1-4\theta_1\theta_2(1-G_{12})\right]^{1/2}} \tag{14}$$

where θ_i is the overall surface area fraction of component i defined as $\theta_i \equiv N_i zq_i / Nzq$ and the energy factor G_{12} is defined by

$$G_{ij} \equiv \exp(\alpha\Delta\delta\tilde{\varepsilon}) \tag{15}$$

$$(\Delta\delta\tilde{\varepsilon} = \delta\tilde{\varepsilon}_{11} + \delta\tilde{\varepsilon}_{22} - 2\delta\tilde{\varepsilon}_{12})$$

where N_i and N represent the number of component i and the total number of molecules, respectively. In Equation (15), α is introduced to represent the degree of non-randomness, that is previously introduced in the NRTL equation [33]. The additional correlation to define the non-randomness factor is given by

$$\Gamma_{ii} = \frac{1-\sum_{j\neq i}\theta_j\Gamma_{ij}}{\theta_i} \tag{16}$$

where $\Gamma_{ij}(i \neq j)$s are considered to be independent variables. Substitution of Equation (16) into Equation (12) gives the right expression for the non-random contribution.

2.3. *Correlation the MDL-NR model to the OCV equation*

The salt activity of the given system is $\ln a = \Delta\mu/kT$. To correlate the MDL-NR model to the OCV equation, the chemical potential is replaced by sum of Equations (8) and (12). For the concentration cells, OCV is given

$$(\Phi^\beta - \Phi^\alpha) = \frac{vRT}{z_+v_+F}\int_\alpha^\beta (1-t_+^0)\left(\frac{\mathrm{d}\ln a_\pm}{\mathrm{d}\ln c_s}\right)\mathrm{d}\ln c_s \tag{17}$$

where α and β are electrolytes of different concentration and Φ^x represents the voltage of x phase. If the

concentration dependence of the transport number is ignored, Equation (17) is reduced to

$$(\Phi^{\beta} - \Phi^{\alpha}) = \frac{vRT}{z_+ v_+ F}(1 - t_+^0) \ln \frac{(a_{\pm})_{\beta}}{(a_{\pm})_{\alpha}} \tag{18}$$

2.4. *The melting point depression theory*

In a semi-crystalline system, the condition of equilibrium between a crystalline polymer and the polymer unit in the solution may be described as follows [20]:

$$\mu_u^c - \mu_u^0 = \mu_u - \mu_u^0 \tag{19}$$

where μ_u^c, μ_u, and μ_u^0 are chemical potentials of the crystalline polymer segment unit, liquid (amorphous) polymer segment unit and chemical potential in the standard state, respectively. Now the chemical potential difference of the crystalline polymer unit appearing on the left-handed side in Equation (19) is correlated to the thermodynamic properties as follows:

$$\mu_u^c - \mu_u^0 = -\Delta H_u (1 - T/T_m^0) \tag{20}$$

where ΔH_u is the heat of fusion per segment unit, T_m and T_m^0 are melting point temperatures of the species in the mixture and a pure phase, respectively. The right-hand side of Equation (19) can be restated as follows:

$$\mu_u - \mu_u^0 = \frac{V_u}{V_1}\frac{r_1}{r_2}\left(\frac{\partial \Delta A}{\partial N_2}\right)_{T,V,N_1} \tag{21}$$

where V_1 and V_u are the molar volumes of the salt and of the repeating unit, respectively. By substituting Equations (20) and (21) into Equation (19) and replacing T by $T_{m,2}$, the equilibrium melting temperature of the mixture is given by

$$\frac{1}{T_{m,2}} - \frac{1}{T_{m,2}^0} = -\frac{k}{\Delta H_u}\frac{V_u}{V_1}\frac{r_1}{r_2}\left(\frac{\mu_2 - \mu_2^0}{kT_{m,2}}\right) \tag{22}$$

The subscripts 1, 2 and u refer to the salt, the polymer, and polymer segment unit, respectively. Similarly, we obtain for the salt (component 1)

$$\frac{1}{T_{m,1}} - \frac{1}{T_{m,1}^0} = -\frac{k}{\Delta H_1}\left(\frac{\mu_1 - \mu_1^0}{kT_{m,1}}\right) \tag{23}$$

3. Results and discussion

Figure 1a shows the phase behavior of the PEO/ $LiCF_3SO_3$ system. Dark circles are experimental data for the salt rich phase and triangles are for the polymer rich phase reported by Minier et al. [34]. The solid line is the calculated coexistence curve by the proposed model. The crystalline complex melting curve is calculated from Equation (23), and the polymer melting curve is calculated from Equation (22). Table 1 gives pure literature

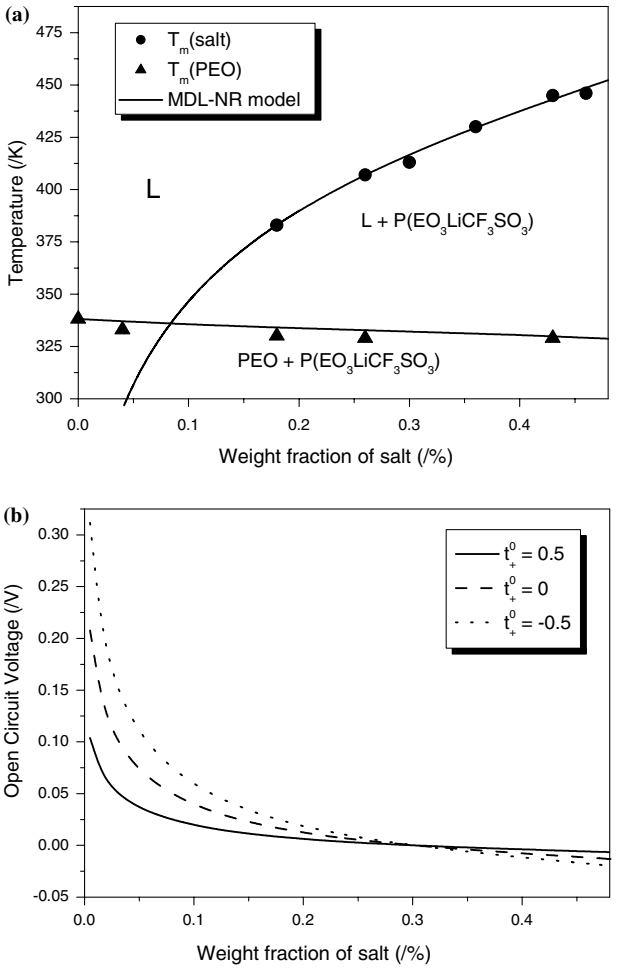

Fig. 1. (a) Phase diagram for the PEO/ $LiCF_3SO_3$ system. The dark circles and triangles are experimental melting point data reported by Minier et al. [34]. The solid lines are calculated by the MDL-NR model. (b) OCV of the concentration cell having the form Li | $PEO_nLiCF_3SO_3$ | $PEO_mLiCF_3SO_3$ | Li calculated by the proposed model at 85 °C.

data of various PEO/salt systems and model parameters for the given systems are listed in Table 2. We let the number of the salt segment, r_1, be a unity and calculate the number of polymer units, r_2, using molar volumes V_1 and V_2 for solvent and polymer, respectively,

$$r_2 = \frac{M_2 V_2}{M_1 V_1} \tag{24}$$

where M_1 and M_2 are molecular masses for salt and polymer, respectively. We set $\eta = 0.3$ and $z = 6$ as suggested by Hu et al. [35]. This phase diagram shows the presence of a eutectic composition at the salt weight % of 0.08. The advantage of using the MDL-NR model is that it gives a comparatively better description of experimental data than those of other model for the given systems, specifically near the eutectic point [28]. Using Equation (18) with parameters obtained from this phase diagram, the concentration cell diagram is calculated hypothetically at the salt weight % of the reference electrolyte ≈ 0.3 with various values of t_+^0. (Figure 1b).

Table 1. Physical properties of polymer and salts

	T_m^0 (/K)	H (J mol^{-1})	M.W (g mol^{-1})	Density (g cm^{-3})	V_u (cm^3 mol^{-1})
PEO	338.15	8284.32[a]	900,000	1.21	36.60
$LiCF_3SO_3$	499.29	10516.48	156.01	2.69	52.66
$ZnBr_2$	667.15	10466.82	225.19	4.20	53.60
$NaCF_3SO_3$	527.15	10554.85	172.06	1.13	36.00
LiTFSI	511.15	–	287.08	1.40	141.90

a : 8284.32*J unit^{-1}.

Table 2. Model parameters for the given systems

	ε/k (/K)	$\delta\varepsilon_{12}/k$ (/K)	α	t_+^0
PEO/$LiCF_3SO_3$	− 12.477	1825.082	0.055	–
PEO/$ZnBr_2$	−197.412	7037.662	0.036	–
PEO/$NaCF_3SO_3$	−228.843	2924.34	0.029	0.439
PEO/LiTFSI	−204.225	3580.72	0.185	0.327

Negative t_+^0 values are best understood in the context of Spiro's definition of transport number [36]. They indicate that negatively charged species, such as triplets containing two anions and one cation that are commonly present in non-ideal solutions, are more mobile than free cations (or positively charged ionic aggregates). These negatively charged species, however, move in the wrong direction under the influence of current (i.e., they move toward the positive electrode during cell charge and vice versa). Better performance can be obtained simply by decreasing the initial salt concentration in the polymer solution to a range where t_+^0 is less negative.

The same procedure is conducted for the PEO/$ZnBr_2$ system for which data were reported by Kim and Bae [37], and OCV curves are calculated and shown in Figure 2. It is well known that PEO forms a stable complex with divalent cations [38]. The eutectic composition, therefore, has a higher value of salt weight % than that of the PEO/ $LiCF_3SO_3$ system as shown in Figure 2. When comparing the calculated OCV values of the two systems, PEO/$LiCF_3SO_3$ system has higher values of OCV than those of the PEO/$ZnBr_2$ system at the same t_+^0. This is because the former system has higher conductivity than that of the latter.

Figure 3a shows the OCV data of concentration cells of the form Na | PEO_n Sodium trifluorosulfonate ($NaCF_3SO_3$) | $PEO_mNaCF_3SO_3$ | Na at 85 °C as a function of the salt weight % where that of the reference electrolyte is near 0.3 [39]. The solid line is calculated by the MDL–NR model and adjustable model parameters are in Table 2. The conductivity and diffusion coefficients of PEO/$NaCF_3SO_3$ system are similar in magnitude to those of PEO/$LiCF_3SO_3$ [40], and this agrees with our result if the two systems have similar values of t_+^0. We represent the hypothetical phase diagram of the PEO/$NaCF_3SO_3$ system using the same activity parameters (Figure 3b). This phase diagram shows a general tendency of melting point depression in polymer/salt electrolyte. The eutectic point is expected to exist at a salt weight % of 0.05. The point shows a lower value than that of the PEO/$LiCF_3SO_3$ system because the molecular weight of PEO in this system is larger by one

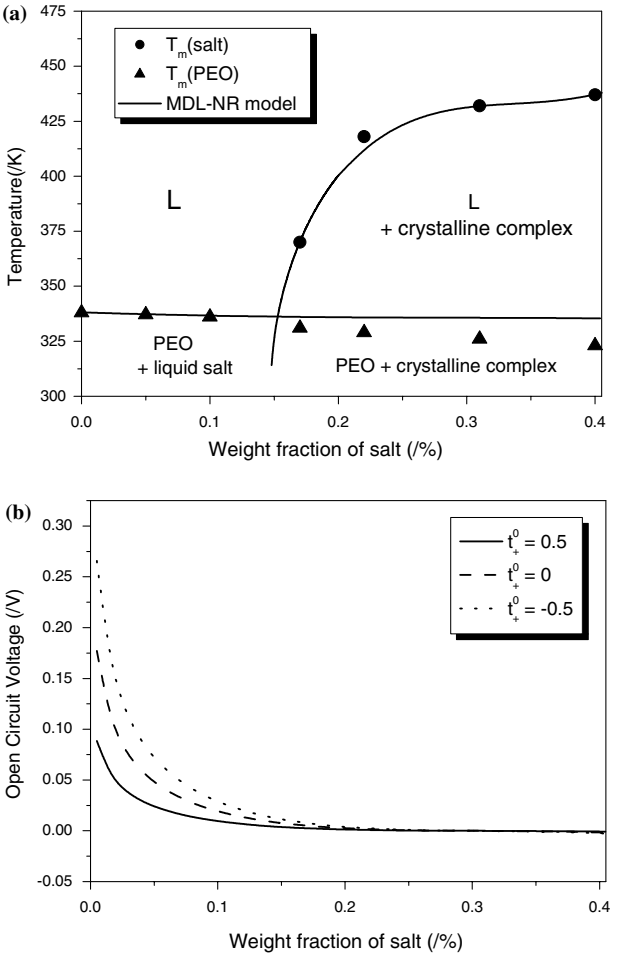

Fig. 2. (a) Phase diagram for the PEO/$ZnBr_2$ system. The dark circles and triangles are experimental melting point data reported by Kim et al. [36]. The solid lines are calculated by the MDL-NR model. (b) OCV of the concentration cell having the form Zn | PEO_nZnBr_2 | PEO_mZnBr_2 | Zn calculated by the proposed model at 85 °C.

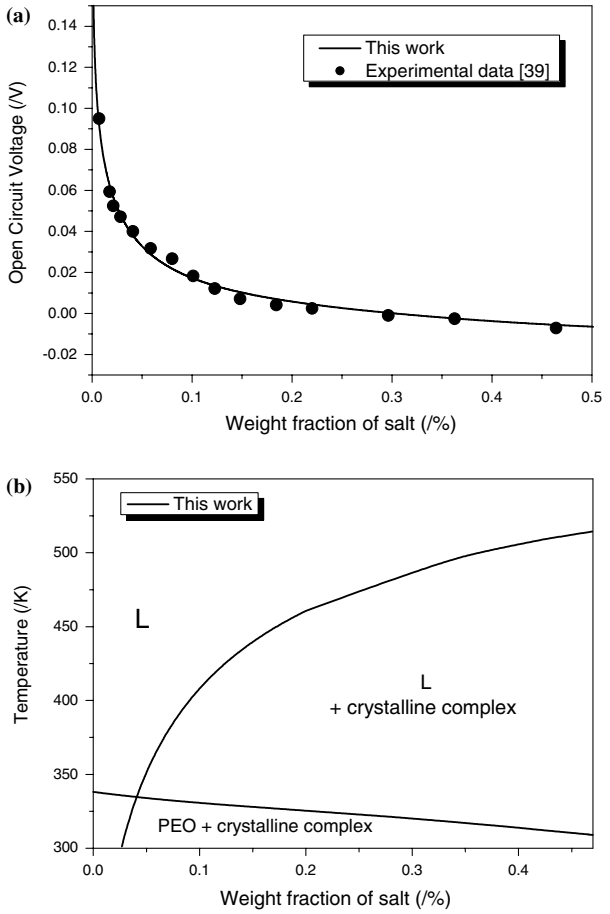

Fig. 3. (a) OCV of the concentration cell having the form Na | $PEO_nNaCF_3SO_3$ | $PEO_mNaCF_3SO_3$ | Na at 85 °C. The dark circles are experimental OCV reported by Ma et al. [39], and the solid line is calculated by the proposed model. (b) Phase diagram for PEO/$NaCF_3SO_3$ system calculated by the MDL-NR model.

order of magnitude. According to the reported data by Ma et al. [39], the maximum of the ionic conductivity appears near the salt weight % of 0.13. This result agrees with the fact that the salt weight % of the maximum ionic conductivity is shifted from the eutectic point to the more concentrated phase, which is also shown in other systems [41].

Figure 4 shows the dependence of the OCV for the concentration cell form Li | PEO_n Lithium bis-trifluoromethanesulfonate imide (LiTFSI) | PEO_mLiTFSI | Li at 85 ° [42]. LiTFSI is reported to act as a plasticizer when complexed with PEO [43]. As with the case of the PEO/$NaCF_3SO_3$ system, the solid line is calculated by the proposed model and the parameters are also given in Table 2. The salt weight % of the reference electrolyte is near 0.3.

4. Conclusion

We establish a new OCV model combining the concentrated solution theory with the MDL-NR model that describes the salt activity in the polymer electrolyte. The proposed model appears to be useful for representing both OCVs and phase diagrams of various PEO/salt systems. Model parameters are determined from phase diagrams of the given systems and used directly to calculate OCV values with one additional parameter, transport number. The advantage of the proposed model follows from its simplicity and accuracy.

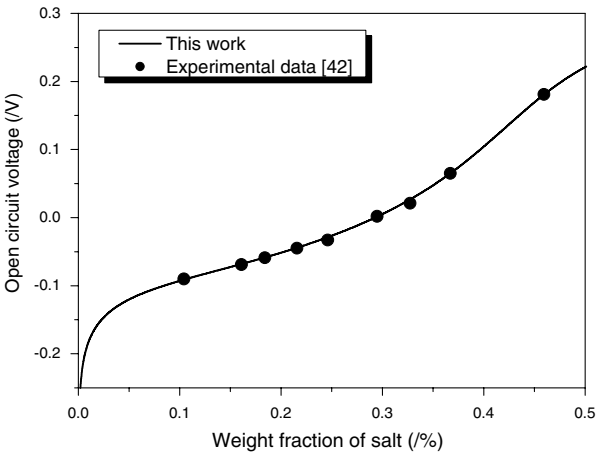

Fig. 4. Open circuit voltage of concentration cell having the form Li | $PEO_nLiTFSI$ | $PEO_mLiTFSI$ | Li at 85 °C. The dark circles are experimental OCV reported by Ludvig et al. [42], and the solid line is calculated by the proposed model.

Acknowledgement

This work was supported in part by the Ministry of Information & Communication of Korea ('Support Project of University Information Technology Research Center' supervised by IITA)

References

1. P.V. Wright, *Br. Polym. J.* **7** (1975) 319.
2. K. Marata, S. Izuchi and Y. Yoshihisa, *Electrochim. Acta* **45** (2000) 1501.
3. M.M. Doeff, A. Ferry, Y.P. Ma, L. Ding and L.C. DeJonghe, *J. Electrochem. Soc.* **144** (1997) L20.
4. M. Doyle, T.F. Fuller and J. Newman, *J. Electrochem. Soc.* **140** (1993) 1526.
5. M. Doyle, J. Newman, A.S. Gozdz, C.N. Schmutz and J.M. Tarascon, *J. Electrochem. Soc.* **143** (1996) 1890.
6. M. Doyle and J. Newman, *Electrochim. Acta* **39** (1995) 2073.
7. J. Newman, Electrochemical Systems (Prentice Hall, Englewood Cliffs, NJ, 1991).
8. P.G. Bruce, J. Evans and C.A. Vincent, *Solid State Ionics,* **28** (1988) 918.
9. P.G. Bruce, M.T. Hardgrave and C.A. Vincent, *Electrochim. Acta* **37** (1992) 1517.
10. G.G. Cameron, J.L. Harvie and M.D. Ingram, *Solid State Ionics* **34** (1989) 65.
11. L. Christie, A.M. Christie and C.A. Vincent, *Electrochem. Solid State Lett.* **2** (1999) 187.

12. H.L. Dai and T.A. Zawodzinski, *J. Electrochem. Soc.* **143** (1996) L107.
13. H.P. Fritz and A. Kuhn, *J. Power Sources* **41** (1993) 253.
14. P.R. Sörensen and T. Jacobsen, *Electrochim. Acta* **27** (1982) 1671.
15. H.J. Walls and T.A. Zawodzinski, *Electrochem. Solid State Lett.* **3** (2000) 321.
16. M. Watanabe, S. Nagano, K. Sanui and N. Ogata, *Solid State Ionics* **28** (1988) 911.
17. M. Watanabe, M. Rikukawa, K. Sanui and N. Ogata, *J. Appl. Phys.* **58** (1985) 736.
18. J. Xu and G.C. Farrington, *J. Electrochem. Soc.* **143** (1996) L44.
19. M. Doyle, T.F. Fuller and J. Newman, *Electrochim. Acta* **39** (1994) 2073.
20. P.J. Flory, Principles of Polymer Chemistry (Cornell University Press, 8th edn. 1971).
21. P. Smith and A.J. Pennings, *J. Polym. Sci.* **15** (1977) 523.
22. C.C. Gryte, H. Berghmans and G. Smets, *J. Polym. Sci.* **17** (1979) 1295.
23. R.M. Myasnikova, E.F. Titova and E.S. Obolonkova, *Polymer* **21** (1980) 403.
24. J.Y. Kim, S.T. Noh and Y.C. Bae, *Polymer* **39** (1998) 3473.
25. W.Y. Ahn and Y.C. Bae, *Electrochimica Acta* **45** (2000) 3157.
26. Y.S. Choi and Y.C. Bae, *Solid State Ionics* **158** (2003) 243.
27. P. Georen and G. Lindbergh, *Electrochim. Acta* **27** (2001) 577.
28. S.J. Pai and Y.C. Bae, *J. Appl. Polym. Sci.* **94** (2004) 231.
29. R.B. Bird, W.E. Stewart and E.N. Lightfoot, Transport Phenomena (Wiley, New York, 1960).
30. J. Newman and W. Tiedemann, *AIChE J.* **21** (1975) 25.
31. J.S. Oh and Y.C. Bae, *Polymer* **39**(5) (1997) 1149.
32. C. Panayiotou and J.H. Vera, *Fluid Phase Equil.* **5** (1980) 55.
33. H. Renon and J.M. Prausnitz, *AIChE J.* **14** (1968) 135.
34. M. Minier, C. Berthier and W. Gorecki, *J. Phys.* **45** (1984) 739.
35. Y. Hu, S.M. Lambert, D.S. Soane and J.M. Prausnitz, *Marcromolecules* **24** (1991) 4356.
36. M. Spiro, *in* A. Weissberger and B.W. Rossiter (Eds) Techniques of Chemistry, Vol. 1, Part 1A (Wiley, New York, 1970).
37. J.Y. Kim and Y.C. Bae, *Polymer* **40** (1999) 1979.
38. R. Hug, A.R. McGhie and G.C. Farrington, 1st International Symposium on Polymer Electrolytes, St Andrews, UK, June 1987.
39. Y. Ma, M. Doyle, T.F. Fuller, M.M. Doeff, L.C. DeJonghe and J. Newman, *J. Electrochem. Soc.* **142** (1995) 1859.
40. M. Dakihana, S. Schantz and L.M. Torell, *J. Chem. Phys.* **92** (1990) 6271.
41. J.Y. Kim and Y.C. Bae, *Fluid Phase Equil.* **163** (1999) 291.
42. L. Edman, M.M. Doeff, A. Ferry, J. Kerr and L.C. DeJonghe, *J. Phy. Chem. B* **104** (2000) 3476.
43. A. Vallée, S. Besner and Prud'homme, *J. Electrochim. Acta* **37** (1992) 1579.